Patient-specific Modeling of the Heart: Applications to Cardiovascular Disease Management

Razvan Ionasec[1,2], Ingmar Voigt[1,3], Viorel Mihalef[1], Saša Grbić[1,2], Dime Vitanovski[1,3], Yang Wang[1], Yefeng Zheng[1], Joachim Hornegger[3], Nassir Navab[2], Bogdan Georgescu[1], and Dorin Comaniciu[1]

[1] Integrated Data Systems, Siemens Corporate Research, Princeton, USA
[2] Computer Aided Medical Procedures, Technical University Munich, Germany
[3] Pattern Recognition Lab, Friedrich-Alexander-University, Erlangen, Germany

Abstract. As decisions in cardiology increasingly rely on non-invasive methods, fast and precise image analysis tools have become a crucial component of the clinical workflow. Especially when dealing with complex cardiovascular disorders, such as valvular heart disease, advanced imaging techniques have the potential to significantly improve treatment outcome as well as to reduce procedure risks and related costs. We are developing patient-specific cardiac models, estimated from available multi-modal images, to enable advanced clinical applications for the management of cardiovascular disease. In particular, a novel physiological model of the complete heart, including the chambers and valvular apparatus is introduced, which captures a large spectrum of morphological, dynamic and pathological variations. To estimate the patient-specific model parameters from four-dimensional cardiac images, we have developed a robust learning-based framework. The model-driven approach enables a multitude of advanced clinical applications. Gold standard clinical methods, which manually process 2D images, can be replaced with fast, precise, and comprehensive model-based quantification to enhance cardiac analysis. For emerging percutaneous and minimal invasive valve interventions, cardiac surgeons and interventional cardiologists can substantially benefit from automated patient selection and virtual valve implantation techniques. Furthermore, the complete cardiac model enables for patient-specific hemodynamic simulations and blood flow analysis. Extensive experiments demonstrated the potential of these technologies to improve treatment of cardiovascular disease.

1 Introduction

Decisions in cardiovascular disease management increasingly rely on non-invasive imaging, with echocardiography currently regarded as the key evaluation technique. Precise morphological and functional knowledge about the cardiac apparatus is highly appreciated today and considered as a prerequisite for the entire clinical workflow including diagnosis, therapy-planning, surgery or percutaneous

intervention as well as patient monitoring and follow-up [1]. Nevertheless, most non-invasive investigations to date are based on two-dimensional images, user-dependent processing and manually performed, potentially inaccurate measurements [2].

The quality of acquired information, as well as the accessibility and cost effectiveness of each medical imaging modality has radically improved over the past decades. Techniques like Transesophageal Echocardiography (TEE), cardiac Computed Tomography (CT) and Cardiovascular Magnetic Resonance (CMR) imaging, enable dynamic four dimensional scanning of a beating heart over the whole cardiac cycle. Such volumetric time-resolved data encode rich structural and dynamic information, which however is barely exploited in clinical practice, due to its size and complexity as well as the lack of appropriate medical systems.

We developed a novel patient-specific modeling framework of the complete heart from multi-modal cardiac images to facilitate the management of cardiovascular disease. Our methodology relies on a physiological model of the cardiac apparatus, which includes an explicit representation of the heart valves, and captures anatomical, dynamical and pathological variations. To extract patient-specific parameters from four-dimensional data, we developed a robust and efficient discriminative learning-based system. The estimation is formulated as a multi-scale problem through which models of increasing complexity are progressively learned. Based on the patient-specific cardiac modeling techniques, we developed applications that support the clinical workflow including: comprehensive quantitative analysis, automated patient selection and risk stratification, therapy simulation for percutaneous procedures, and computational fluid dynamics for blood flow analysis. The developed machine learning algorithms and performed clinical experiments are backed by a large database of medical images acquired with CT, Ultrasound and MRI scanners, from 476 patients affected by a large spectrum of cardiovascular diseases.

2 Physiological Modeling and Parametrization

We developed a comprehensive model of the heart, which includes the chambers (left ventricle, left atrium, right ventricle and right atrium) [3] and the heart valves (aortic, mitral, tricuspid and pulmonary valves) [4, 5] to capture a large variety of morphological, functional and pathological variations. A modular and hierarchical approach was used to reduce anatomical complexity and facilitate an effective and flexible estimation of individual anatomies. Our model is anatomically-compliant and maintains a consistent parameterization across the cardiac cycle and different patients by utilizing physiological-driven constraints and sampling schemes.

2.1 Parametrization

The global dynamic variation of each heart chamber and valve is parameterized as a temporal dependent similarity transform, which defines the translation, the

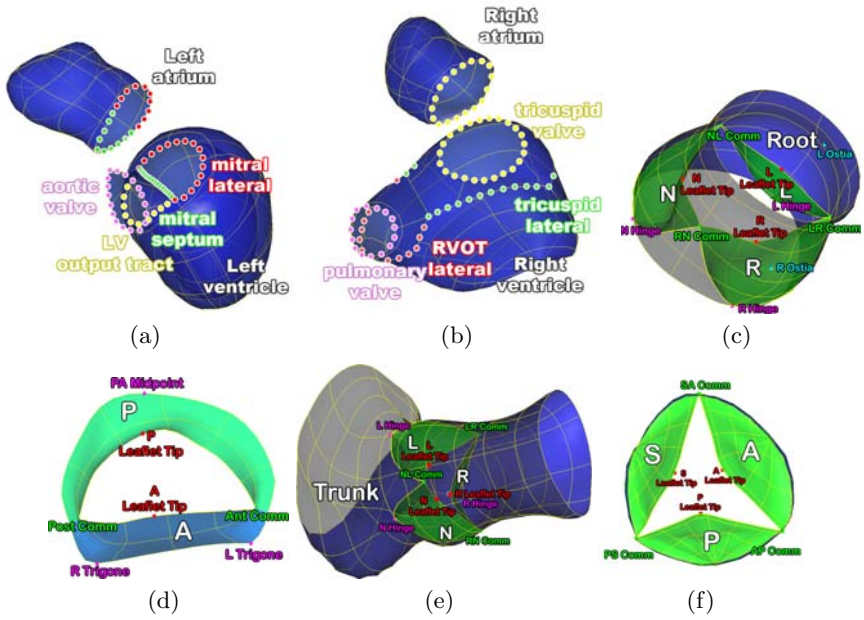

Fig. 1. Cardiac model components: (a) the left heart (left ventricle and left atrium), (b) right heart (right ventricle and right atrium), (c) aortic valve, (d) mitral valve, (e) pulmonary valve and (f) tricuspid valve.

quaternion representation of the rotation, the similarity transform scaling factors, and the temporal position in the cardiac cycle. A set of 152 anatomical landmarks for the heart chambers and 33 for the valves, described in the next paragraph, are used to parameterize the complex and synchronized motion pattern of all heart anatomies. Thereby, each landmark is described by a trajectory in a three dimensional space, normalized by the temporal dependent similarity transform. The final model is completed with a set of 9 dense surface meshes to represent the chambers and an additional set of 13 structures for the valves. Each mesh is sampled along anatomical grids of vertices defined through the landmarks [3, 4].

2.2 Anatomical Definition

Left ventricle and atrium: The left ventricle is constructed from 78 landmarks (16 mitral lateral, 15 mitral septum, 16 left ventricle output tract and 32 aortic valve control points) and four surface geometries (LV epicardium, LV endocardium and LV output tract). The left atrial surface is connected to it's ventricle via the aortic valve control points (Fig. 1(a)) [3].
Right ventricle and atrium The right ventricle is composed of 74 landmarks (16 tricuspid lateral, 15 tricuspid septum, 28 tricuspid valve and 18 pulmonary valve control points) and four surface geometries (RV apex, RV output tract

and RV inflow tract). The right atrial surface is constrained by 28 tricuspid valve control points and links to the right ventricle (Fig. 1(b)) [3].
Aortic valve: The aortic valve consists of 11 landmarks (3 commissures, 3 hinges, 3 leaflet tips and 2 ostias) and four surface structures (aortic root, N-, L- and R-leaflet). The aortic root is constrained by the hinge and commissure plane and each leaflet is spanned between two commissures and one hinge (Fig. 1(c)) [4].
Mitral valve: The mitral valve is composed of 7 landmarks (3 trigones, 2 commissures and 2 leafleat tips). The anterior leaflet is defined by two trigones, one leaflet tip and two commissures and the posterior leaflet by three trigones, one leaflet tip and one commissure (Fig. 1(d)) [4].
Pulmonary valve: The pulmonary valve is consisting of 9 landmarks (3 commissures, 3 hinges and 3 leaflet tips) and four surface structures (pulmonary root, N-, L- and R-leafet) (Fig. 1(e)) [6].
Tricuspid valve: The tricuspid valve is constructed from four surface geometries (annulus, septal-, anterior- and posterior leaflet) and six anatomical landmarks (three commissures and three leaflet tips) (Fig. 1(f)) [5].

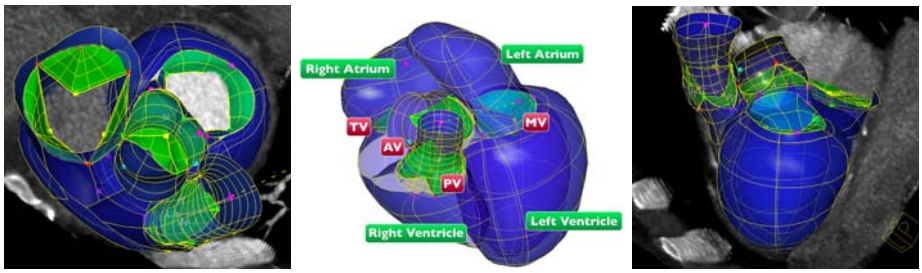

Fig. 2. Examples of personalized model estimated from a multiphase CT sequence.

3 Patient-specific Parameter Estimation

We developed a robust learning-based framework to estimate the patient-specific parameters of the previously introduced heart model from four-dimensional data. To guarantee robustness against image artifacts and handle the shape and appearance variations encountered in cardiac images, our approach relies on boosting techniques, in particular the Probabilistic Boosting Tree (PBT) [7]. Computation speed is essential to qualify novel technologies for clinical practice. Thus, we developed search space marginalization methods, such as the Marginal Space Learning (MSL) [3] and Trajectory Spectrum Learning (TSL) [8, 4], to efficiently perform optimization in multi-dimensional parameter domains.

To handle the problem complexity, the estimation is following a coarse-to-fine strategy based on the natural level of detail of the underlining anatomies. The input data is a temporal sequence of volumetric scans acquired with one

of the three modalities: CT, Ultrasound or MRI. The natural first step is to recover the pose and corresponding motion parameters of each model component from the input cardiac data. Through a novel approach, which combines MSL [3] with RANSAC techniques, we obtained robust and time-coherent object localization [4]. In the second step, the anatomical landmarks' location and motion are simultaneously estimated using the TSL algorithm [8], which employs trajectory-based features and strong trajectory spectrum classifiers. The final stage tackles the boundary delineation of the complete heart surfaces over the entire cardiac cycle. Our method leverages robust boundary detectors together with collaborative trackers and motion manifolds [9].

On average, the precision of the patient-specific estimation is 1.73mm at a speed of 4.8sec per volume for the valvular model and 1.13-1.57mm at a speed of 4.0sec for the chambers. We demonstrated that our automated method is robust with respect to different image modalities and the obtained accuracy is within the inter-user variability.

4 Clinical Applications

In the remainder of this paper we leveraged the patient-specific cardiac model obtained from multiple image modalities to demonstrate a variety of non-invasive analysis procedures, which can lead to reduced therapeutical costs and complication risks, as well as improved treatment outcome.

4.1 Quantitative and Qualitative Analysis

Precise quantification of the anatomy and function is fundamental in the medical management of cardiovascular disease. The clinical gold standard still processes 2D images and performs manual measurements which are tedious to obtain and moreover known to be affected by inaccuracies [2].

We proposed a paradigm shift in the clinical evaluation of the cardiac apparatus, which aims to replace manual analysis based on 2D images with automated model-based quantification from 4D data. The explicit mathematical model is exploited to express a wide-ranging collection of quantitative parameters that support the overall clinical decision making process. In the following we present a selection of clinical experiments.

Valves Analysis: Table 1 presents the system-precision for various dimensions of the aortic-mitral coupling: diameters of the ventricular-arterial junction (VAJ), sinus of valsalva (SV) and sinotubular junction (SJ), aortic valve area (AV area), mitral valve area (MV area), mitral annular circumference (AC) , anteroposterior diameter (APD), anterolateral-posteromedial diameter (AL-PM-D) [4].

Chambers Analysis: The motion pattern of a chamber during a cardiac cycle provides many important clinical measurements of its functionality, e.g., the ventricular ejection fraction, myocardium wall thickness, and dissynchrony within a chamber or between different chambers [3].

	Mean	STD
VAJ (cm)	0.137	0.017
SV (cm)	0.166	0.043
STJ (cm)	0.098	0.029
AC (cm)	0.846	0.3
APD (cm)	0.325	0.219
AL-PM-D(cm)	0.509	0.37

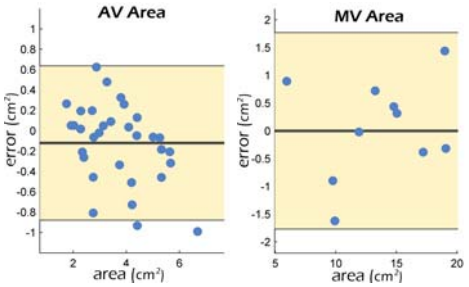

Table 1. Precision for various dimensions of the aortic-mitral coupling along with Bland- Altman plots for the aortic valve area and mitral annular area. The aortic valve experiments were performed on CT data from 36 patients, while the mitral valve was evaluated on TEE data from 10 patients, based on the input of expert cardiologists.

The benefits of the proposed model-based analysis are: **Precision** - increased by robust modeling and measuring the natural three-dimensional valve anatomy, **Efficiency** - by automated quantification that outperforms manual measuring in terms of required analysis time, and **Comprehensiveness** - through analysis that includes four-dimensional information of the morphology and function of the entire cardiac apparatus.

4.2 Computer Aided Diagnosis and Case Retrieval

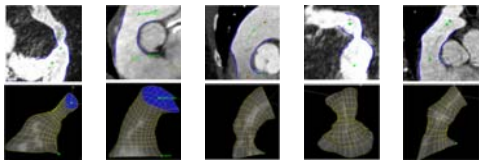

Fig. 3. Types of pulmonary trunk morphologies: (a) pyramidal shape, (b) constant diameter, (c) inverted pyramidal shape, (d) narrowed centrally but wide proximally and distally, (e) wide centrally but narrowed proximally and distally.

Clinical decisions are largely based on generic information and rule sets from clinical guidelines and publications, and personal experience of clinicians. Besides investigating the quantitative capabilities of our cardiac models, we also proposed a generic method on how to automatically derive high-level clinical information using learning-based discriminative distance functions [10]. We formulate inference in a comprehensive feature space, which incorporates the complex morphologic and functional information. Generally we address two tasks: retrieval of similar cases using a learned distance function, which measures the

similarity of two particular cardiac shapes, and a binary classification problem, based on geometric models and derived features.

For distance learning we considered two techniques, namely learning from equivalence constraints and the intrinsic Random Forest distance. Equivalence constraints are represented using triplets of two model instances' feature vectors and a label indicating whether the two instances are similar or dissimilar. Learning from these triplets is often called learning in the product space and demonstrated to be effective for high dimensional data with many correlated, weakly relevant and irrelevant features [10]. The signed margin of models constructed using boosting or Random Forests is used as the required distance function for our experiments with equivalence constraints.

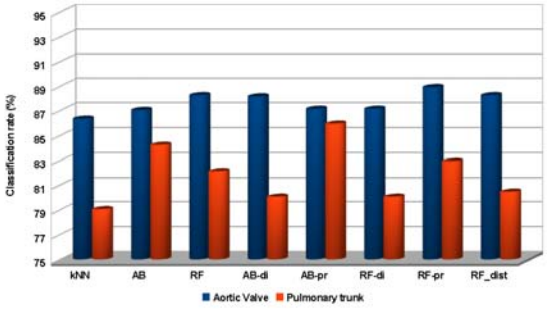

Fig. 4. Classification accuracy for the different learning techniques applied to Aortic Valve Disease classification and PPVI suitability selection.

The generic approach enables learning arbitrary user-defined concepts of similarity depending on the application. This is demonstrated with two applications: 1) diagnosis and severity assessment of aortic valves and 2) patient selection for Percutaneous Pulmonary Valve Implantation (PPVI), where classification rates of up to 88.9% and 85.9% could be observed on a set of valve models from 288 and 102 patients respectively (Fig. 4). The morphology of the pulmonary trunk is a major determinant of suitability for PPVI [6]. Intervention in unsuitable patients exposes them to unnecessary invasive catherization. In the classification scheme depicted in Fig. 3 patients from type (a) are considered to be unsuitable for PPVI due to the narrow artery and high probability of device migration. Shape features extracted from the estimated pulmonary trunk are used to learn a discriminative distance function to discriminating anatomies of type (a) from other classes.

4.3 Computational Decision Support for Percutaneous Procedures

Percutaneous approaches are becoming increasingly popular, due to reduced procedural complications and lower follow-up rates [1]. The prosthetic implants are delivered through catheters using transvenous, transarterial or transapical

Fig. 5. Schematic description of the proposed computational decision support workflow for percutaneous aortic valve implantation.

techniques, which obstructs clinicians from a direct view and access to the affected anatomies. Thus, the success of the intervention relies to a large portion on intra-operative images, and the experience and skills of the operator, while a suboptimal deployment location can result in poor hemodynamic performance with severe paravalvular leakages and/or high gradients and suboptimal effective orifice.

We proposed a novel framework for preoperative planning, intraoperative guidance and post-operative assessment of percutaneous aortic valve replacement procedures with stent mounted devices (Fig. 5) [11]. Our model of the aortic valvular complex including aortic valve and aorta ascendens is used to perform an in-silico delivery of the valve implant based on deformable simplex meshes and geometrical constraints. The device is modeled out of the *stent mesh*, which precisely mimics the geometry of the prosthesis and the *computational mesh*, a superimposed 2-simplex mesh, which is used to guide the expansion. The expansion of the device is modeled by balancing external and internal forces as encountered in the actual procedure, using iterative optimization methods (Fig. 6). The deformation is described by a finite difference discretization of a second order differential equation.[12].

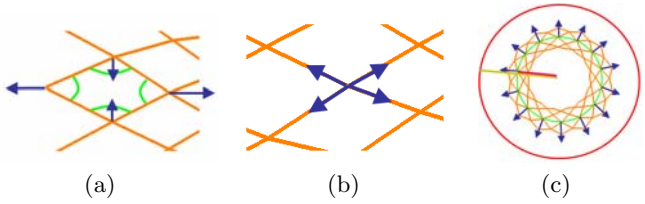

Fig. 6. Forces acting on the model on deployment to converge to the observed geometric properties: (a) f_{angle} enforces the charateristic angles at the strut joints (green), (b) f_{length} maintains the strut lengths. (c) f_{circ} enforces the circumference (green), while f_{ext} dampens and eliminates the all forces acting along the stent mesh normal wheighted by the fraction of distances of strut joint and vessel wall (red) to the stent centroid (magenta/yellow). Please note that (c) shows a short axis cross section of the stent mesh.

The predictive power of the model-based in-silico valve replacement was evaluated on 20 patients with pre- and postoperative 3D cardiac CT scans, each by

comparing the preoperative prediction result with a ground truth model manually fitted to the real device imaged in the postoperative data (Fig. 5). With an accuracy bellow 2mm at the annular level, we demonstrated the potential of this approach to support preoperative planning by finding the best implant type, size and deployment location and orientation via in-silico implantation under various treatment hypotheses until optimal predicted performance is observed.

4.4 Computational Hemodynamics in the Human Heart

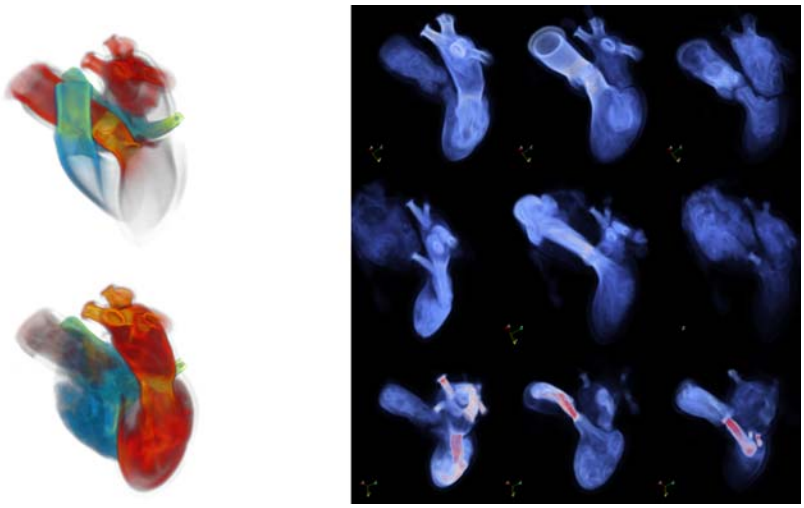

Fig. 7. Left images: visualization of the blood flow vorticity magnitude for whole heart during systole (top) and diastole (bottom). Right images: comparison of diseased hearts. Top: normal heart; Middle: heart with dilated aorta; Bottom: heart with bicuspid valve. First column: peak diastole; Second column: peak systole; Third column: end systole.

By using the patient-specific cardiac model presented in the previous sections as an input to a 3D Navier-Stokes solver, we derive realistic hemodynamics, constrained by the local anatomy, along the entire heart cycle. This enables us to advance the state-of-the-art in two ways: first, we obtain realistic cardiac blood flow computations for the entire heart, and second, we present a differential assessment of the flow dynamics corresponding to specific heart conditions. The flow computations presented here differ in an essential manner from other works: the realistic patient-specific valve models modulate the blood flow significantly, in accordance to the presence of various cardiac pathologies.

For the computations presented here we essentially enforce a one-way transfer of the heart mesh kinematics to the cardiac blood flow, using the framework presented in [13, 14]. The Navier-Stokes equations with viscous terms are solved

in a level set formulation, using a fractional step combined with an approximate projection method for the pressure. The equations are discretized on a uniform grid, using finite difference and finite volume techniques. The heart mesh is immersed in the computational domain with the help of a level set function that effectively "thickens" the original triangle mesh by the grid spacing. The interface location is used to impose no-slip boundary conditions to the fluid region. The mesh velocity, which is known at each time step, is extrapolated to the interfacial nodes using extrapolation kernels.

The blood flow computations inside both the left and right sides of the heart [14] produced flow curve data qualitatively similar to the flow curves presented in the literature. Very interesting was the comparison of the results of the diseased hearts with the normal one (Fig. 7) [13]. The normal heart displayed strong systolic and diastolic fluxes, with blood jets directed toward the center of the aorta, respectively the center of the left ventricle. The two diseased hearts - one with a dilated aortic root and one with a bicuspid aortic valve - displayed quite different flow characteristics. For the heart with a heavily enlarged aorta the aortic valve never closed, leading to massive aortic regurgitation during diastole and a systolic flow directed straight toward the abnormally enlarged region of the aorta. The bicuspid aortic valve also produced a very strong regurgitation at the beginning of the diastole toward the left ventricle, while a sclerotic mitral valve directed the diastolic jet straight toward the posterior ventricular wall.

The flow computations we performed underline the importance of the patient-specific cardiac geometry and especially of the valve apparatus in determining the hemodynamic characteristics. Our first validation efforts for hemodynamics computations [14], which qualitatively compare the flow curves with measured ultrasound ones, will be augmented with direct comparisons of velocity fields determined using phase-contrast MRI.

5 Conclusion

We described our comprehensive heart model, which includes an explicit representation of the valvular apparatus, and parameterizes morphological, functional and pathological variations of the cardiac apparatus. Subsequently, we presented a robust and efficient learning-based framework to estimate patient-specific model parameters from multi-modal cardiac images. Based on several clinical applications, we demonstrated the relevance of the developed technologies to advance the management of cardiovascular disease. Nevertheless, extensions of the model to include tissue and other biomechanical properties, and further anatomical details, such as papillary muscles, chordae tendineae and trabeculations are necessary future developments.

References

1. Otto, C., Bonow, R.O.: Valvular Heart Disease: A Companion to Braunwald's Heart Disease. Saunders (2009)

2. Bonow, R.O., Carabello, B.A., Chatterjee, K., de Leon, A.C.J., Faxon, D.P., Freed, M.D., Gaasch, W.H., Lytle, B.W., Nishimura, R.A., O?Gara, P.T., O?Rourke, R.A., Otto, C.M., Shah, P.M., Shanewise, J.S.: Acc/aha 2006 guidelines for the management of patients with valvular heart disease: a report of the american college of cardiology/american heart association task force on practice guidelines (writing committee to develop guidelines for the management of patients with valvular heart disease). Circulation **114**(5) (2006) 84–231
3. Zheng, Y., Georgescu, B., Barbu, A., Scheuering, M., Comaniciu, D.: Four-chamber heart modeling and automatic segmentation for 3D cardiac CT volumes using marginal space learning and steerable features. IEEE Transactions on Medical Imaging **27**(11) (2008) 1668–1681
4. Ionasec, R.I., Voigt, I., Georgescu, B., Wang, Y., Houle, H., Vega-Higuera, F., Navab, N., , Comaniciu, D.: Patient-specific modeling and quantification of the aortic and mitral valves from 4D cardiac CT and TEE. In: IEEE Transactions on Medical Imaging, in press (2010)
5. Grbic, S., Ionasec, R.I., Vitanovski, D., Voigt, I., Wang, Y., Georgescu, B., Navab, N., Comaniciu, D.: Complete valvular heart apparatus model from 4D cardiac CT. In: Proceedings of MICCAI. (2010)
6. Vitanovski, D., Ionasec, R., Georgescu, B., Huber, M., Taylor, A., Hornegger, J., Comaniciu, D.: Personalized pulmonary trunk modeling for intervention planning and valve assessment estimated from CT data. In: Proceedings of MICCAI. (2009) 17–25
7. Tu, Z.: Probabilistic boosting-tree: Learning discriminative methods for classification, recognition, and clustering. In: International Conference on Computer Vision. (2005) 1589–1596
8. Ionasec, R.I., Wang, Y., Georgescu, B., Voigt, I., Navab, N., Comaniciu, D.: Robust Motion Estimation Using Trajectory Spectrum Learning: Application to Aortic and Mitral Valve Modeling from 4D TEE. In Society, I.C., ed.: Proceedings of 12th IEEE International Conference on Computer Vision 2009. (2009) 1601–1608
9. Yang, L., Georgescu, B., Zheng, Y., Meer, P., Comaniciu, D.: 3d ultrasound tracking of the left ventricle using one-step forward prediction and data fusion of collaborative trackers. In: IEEE Conference on Computer Vision and Pattern Recognition. (2008)
10. Voigt, I., Vitanovski, D., Ionasec, R.I., Tsymbal, A., Georgescu, B., Zhou, S.K., Navab, N., Hornegger, J., Comaniciu, D.: Learning discriminative distance functions for valve retrieval and improved decision support in valvular heart disease. In: Proceedings of SPIE Medical Imaging. (2010)
11. Voigt, I., Ionasec, R.I., Georgescu, B., Boese, J., Brockmann, G., Hornegger, J., Comaniciu, D.: Computational Decision Support for Percutaneous Aortic Valve Implantation. In: Proceedings of the 5th International Workshop on Medical Imaging and Augmented Reality. (2010)
12. Larrabide, I., Radaelli, A., Frangi, A.F.: Fast virtual stenting with deformable meshes: Application to intracranial aneurysms. In: Proceedings of MICCAI. (2008) 790–797
13. Mihalef, V., Ionasec, R., Wang, Y., Zheng, Y., Georgescu, B., Comaniciu, D.: Patient-specific modeling of left heart anatomy, dynamics and hemodynamics from high resolution 4D CT. In: Proceedings of ISBI. (2010)
14. Mihalef, V., Ionasec, R., Sharma, P., Georgescu, B., Huber, M., Comaniciu, D.: Patient-specific modeling of whole heart anatomy, dynamics and hemodynamics from 4D cardiac CT images. In: Proceedings of VPH. (2010 (to appear))